J Nanopart Res (2012) 14:884
DOI 10.1007/s11051-012-0884-7

RESEARCH PAPER

Nanofiltration membranes based on polyvinylidene fluoride nanofibrous scaffolds and crosslinked polyethyleneimine networks

Seong-Jik Park · Ravi Kumar Cheedrala · Mamadou S. Diallo · Changmin Kim · In S. Kim · William A. Goddard III

Received: 1 February 2012 / Accepted: 20 April 2012 / Published online: 28 June 2012

Abstract In this article, we describe the synthesis of new and ion-selective nanofiltration (NF) membranes using polyvinylidene fluoride (PVDF) nanofibers and hyperbranched polyethylenimine (PEI) as building blocks. These new nanofibrous composite (NFC) membranes consist of crosslinked hyperbranched PEI networks supported by PVDF nanofibrous scaffolds that are electrospun onto commercial PVDF microfiltration (MF) membranes. A major objective of our study was to fabricate positively charged NF membranes that can be operated at low pressure with high water flux and improved rejection for monovalent cations. To achieve this, we investigated the effects of crosslinker chemistry on membrane properties (morphology, composition, hydrophobicity, and zeta potential) and membrane performance (salt rejection and permeate flux) in aqueous solutions (2,000 mg/L) of four salts (NaCl, $MgCl_2$, Na_2SO_4, and $MgSO_4$) at pH 4, 6, and 8. We found that an NFC–PVDF membrane with a network of PEI macromolecules crosslinked with trimesoyl chloride has a high water flux (~ 30 L m^{-2} h^{-1}) and high rejections for $MgCl_2$ (~ 88 %) and NaCl (~ 65 %) at pH 6 using a pressure of 7 bar. The overall results of our study suggest that PVDF nanofibers and hyperbranched PEI are promising building blocks for the fabrication of high performance NF membranes for water purification.

Special Issue Editors: Mamadou Diallo, Neil Fromer, Myung S. Jhon

This article is part of the Topical Collection on Nanotechnology for Sustainable Development

S.-J. Park · R. K. Cheedrala · M. S. Diallo (✉) · W. A. Goddard III
Graduate School of Energy, Environment, Water and Sustainability (EEWS), Korea Advanced Institute of Science and Technology (KAIST), Daejeon, Republic of Korea
e-mail: mdiallo@kaist.ac.kr; diallo@wag.caltech.edu

Present Address:
S.-J. Park
Department of Bioresources and Rural Systems Engineering, Hankyong National University, Anseong, Greonggi-do 456-749, Republic of Korea

M. S. Diallo
Environmental Science and Engineering, Division of Engineering and Applied Science, California Institute of Technology, Pasadena, CA, USA

C. Kim · I. S. Kim
Department of Environmental Science and Engineering, Gwangju Institute of Science and Technology (GIST), Gwangju, Korea

W. A. Goddard III
Materials and Process Simulation Center, Division of Chemistry and Chemical Engineering, California Institute of Technology, Pasadena, CA, USA

Keywords Nanofibers · Polyethylenimine · Polyvinylidene fluoride · Hyperbranched · Polymer networks · Membranes · Nanofiltration · Water purification · Nanotechnology sustainable development

Introduction

The availability of clean water has emerged as one of the most critical problems facing society and the global economy in the twenty-first century. Many regions of the world are already experiencing higher demands for clean water while freshwater supplies are being stressed (Service 2006; Shannon et al. 2008). According to the World Resources Institute, 40 % of the world's population lives in water-stressed areas. The United Nations Environment Program (UNEP) predicts that freshwater will be scarcer in many regions of the world by 2030 (UNEP 2006). The problem will get much worse unless we develop more efficient, cost-effective and environmentally sound technologies to extract clean water from impaired water including wastewater, brackish water, and seawater (Shannon et al. 2008; Diallo and Brinker 2011). Pressure-driven membrane processes such as reverse osmosis (RO), nanofiltration (NF), ultrafiltration (UF), and microfiltration (MF) have become the key components of advanced water reuse and desalination systems throughout the world. RO is considered as the best commercially available desalination technology (Shannon et al. 2008; Elimelech and Philipp 2011). In RO, a high pressure is applied to force saline water through a semi-permeable membrane that retains salts (e.g., dissolved ions) while allowing the pure water to pass through the membrane. Due to its lower pressure requirements, NF is increasingly being used as alternative to RO in water softening and water reclamation (Schäefer et al. 2005). Today, the vast majority of commercial NF membranes are thin film composite (TFC) membranes with three components (Schäefer et al. 2005): (1) a nonwoven polymeric support [polyethylene terephthalate], (2) a microporous polymeric support [polysulfone], and (3) a thin separation layer consisting of crosslinked polyamide (PA). Commercial TFC-PA NF membranes have small pores (0.5–1.5 nm) and are negatively charged (Schäefer et al. 2005). Because of this, their mechanisms of ion rejection include (i) size exclusion, (ii) Donnan exclusion, and (iii) dielectric exclusion (Vezzani and Bandini 2002; Escoda et al. 2010; Déon et al. 2011). Although TFC-PA NF membranes are effective in most cases at retaining (>95 %) divalent anions (e.g., SO_4^{2-} and PO_4^{3-}), they have limited retention capability for monovalent anions (e.g., Cl^-) and cations (e.g., Na^+) (Schäefer et al. 2005). Thus, there is great need for novel, low pressure and robust NF membranes with enhanced rejection capability for monovalent cations/anions.

Recent advances in nanotechnology such as the fabrication of polymeric nanofibers (PNFs) by electrospinning (ES) are providing unprecedented opportunities to develop a new generation of high performance filtration media and membranes for water purification (Ramakrishina et al. 2005; Yoon et al. 2008). During the last decade, ES has emerged as a versatile technique for synthesizing a broad range of nanofibers including PNFs, inorganic nanofibers, and hybrid polymeric–inorganic nanofibers (Ramakrishina et al. 2005). With ES, polymeric fibers with diameters ranging from 10–100 nm to 1–10 μm can be produced. Electrospun PNFs have several unique characteristics such as large surface area to unit volume, large porosity (up to over 80 %), and versatile chemistry. Several investigators have begun exploiting these unique properties of electrospun PNFs to develop novel MF, UF, and NF membranes for water purification. Gopal et al. (2006) have reported the synthesis of electrospun nanofibrous membranes using polyvinylidene fluoride (PVDF) and polysulfone as base polymers. They showed that these new MF membranes could reject more than 90 % of polystyrene (PS) microparticles (5, 7, 8, and 10 μm in diameter) in solution with high water flux and no significant fouling using a transmembrane pressure of ~0.5 bar. Wang et al. (2005) have reported the fabrication of a new UF membrane consisting of a thin layer of crosslinked poly(vinyl alcohol) nanofibers that were electrospun onto an electrospun polyacrylonitrile (PAN) nanofibrous substrate. Their filtration experiments showed that the new thin film nanofibrous composite (TFNC) UF membrane could separate a model soybean oil–water emulsion with high rejection (99.5 %) and high water flux (210 L m^{-2} h^{-1}) using a pressure of 3 bar. Yoon et al. (2009) have fabricated a new TFNC NF membrane consisting of an electrospun PAN nanofibrous support with a PA layer that was

synthesized by interfacial polymerization of piperazine and bipiperidine. They evaluated the performance of the new membrane using cross-flow filtration of aqueous solutions of $MgSO_4$ (2,000 mg/L) at a pressure of 4.8 bar. Yoon et al. (2009) reported that the $MgSO_4$ rejection (~98 %) of their new TFNFC membrane was comparable to that of the commercial NF270 TFC NF membrane from DOW-FILMTEC™. However, its permeate flux was 38 % higher than that of the NF270 membrane.

Despite these promising results, a great deal of fundamental research remains to be done to advance the basic science and engineering knowledge needed to fabricate viable NF membranes using electrospun PNFs as building blocks (Yoon et al. 2008). A key challenge includes the identification and selection of PNFs with the robust chemical, thermal and mechanical properties and the versatile chemistry required to fabricate high performance NF membranes for water treatment, reuse, and desalination. In this article, we describe the preparation of novel nanofibrous composite (NFC) membranes using PVDF and hyperbranched polyethylenimine (PEI) as building blocks. These new NFC–PVDF–PEI membranes consist of crosslinked hyperbranched PEI networks supported by PVDF nanofibrous scaffolds that are electrospun onto commercial PVDF MF membrane supports (Fig. 1). A key driver of our study was to fabricate positively charged NF membranes with high water flux and improved rejection for monovalent cations. Such membranes are needed to expand the applicability of NF to the treatment/reclamation of acid mine drainage and industrial wastewater contaminated by toxic metal ions (e.g., Cu^{2+}, Zn^{2+}, and Pb^{2+}) and cationic organic compounds (e.g., dye and biopharmaceuticals) (Cheng et al. 2011; Ji et al. 2011; Sun et al. 2011; Ba et al. 2009). In our efforts to develop low pressure, ion selective and positively charged NFC membranes, we investigated the effects of crosslinker chemistry on membrane properties (morphology, composition, hydrophobicity, and zeta potential) and membrane performance (salt rejection and permeate flux). Three crosslinkers were evaluated including trimesoyl chloride (TMC), 1,3-dibromo propane (DBP), and epichlorohydrin (ECH). Four salts (NaCl, $MgCl_2$, Na_2SO_4, and $MgSO_4$) were tested. The overall results of our study suggest that PVDF nanofibers and hyperbranched PEI are promising building blocks for the fabrication of high performance NF membranes for water purification.

Experimental methods and procedures

Materials

PVDF MF membrane supports (0.45 μm pore size) were purchased from Millipore (USA). PVDF powder (Kynar 761) was provided by Arkema (USA). Hyperbranched PEI [M_w: 25,000 and M_n: 10,000] was provided by BASF (Germany). Dimethylformamide (DMF), *n*-methyl-2-pyrrolidone (NMP), TMC, 1,3-DBP, and ECH were purchased from Sigma-Aldrich. Analytical grade NaCl, $MgCl_2$, Na_2SO_4, and $MgSO_4$ were purchased from Samchon Chemicals (Korea). All chemicals were used as received. Deionized (DI) water (18.2 MΩ cm resistivity) was used to rinse the membranes and prepare the salt solutions.

Nanofiber and membrane synthesis

We utilized blends of PVDF + PEI to spin the nanofibrous scaffolds of the NFC–PVDF–PEI membranes. A typical polymer blend was prepared by dissolving PVDF (18.5 wt%) and PEI (2.5 wt%) in a mixture of DMF and NMP (1:1 w/w). The mixture was sonicated for 4 h to obtain a homogeneous PVDF/PEI solution. A NANON-01A ES machine (MECC, Japan) was employed to spin the PVDF nanofibrous scaffold of each membrane. The PVDF MF support was first mounted on the NANON-01A drum collector. Following this, the PVDF/PEI blend was electrospun onto the PVDF membrane support using a solution flow rate of 0.7 mL/h and a voltage of 29 kV. During the ES process, the distance between the needle and the collector drum was kept constant at 7.5 cm. The speed of the collector was also kept constant 500 rpm. After the completion of the ES process, 1.0 mL of a solution of hyperbranched PEI in methanol (50 wt%) was electrosprayed onto the electrospun nanofibrous PVDF membranes using a solution flow rate 0.3 mL/h, a voltage of 29 kV, a needle to collector distance of 7.5 cm, and a collector speed of 2,500 rpm. Table 1 shows the process parameters used to (i) spin the PVDF nanofibers and (ii) spray them with PEI. Following electrospraying, the PEI-coated PVDF nanofibrous scaffolds were reacted with the crosslinkers to generate three different types of membranes (Fig. 1). To synthesize the NFC–PVDF–PEI-1 membranes, the PEI-coated nanofibrous scaffolds were reacted with a solution of TMC

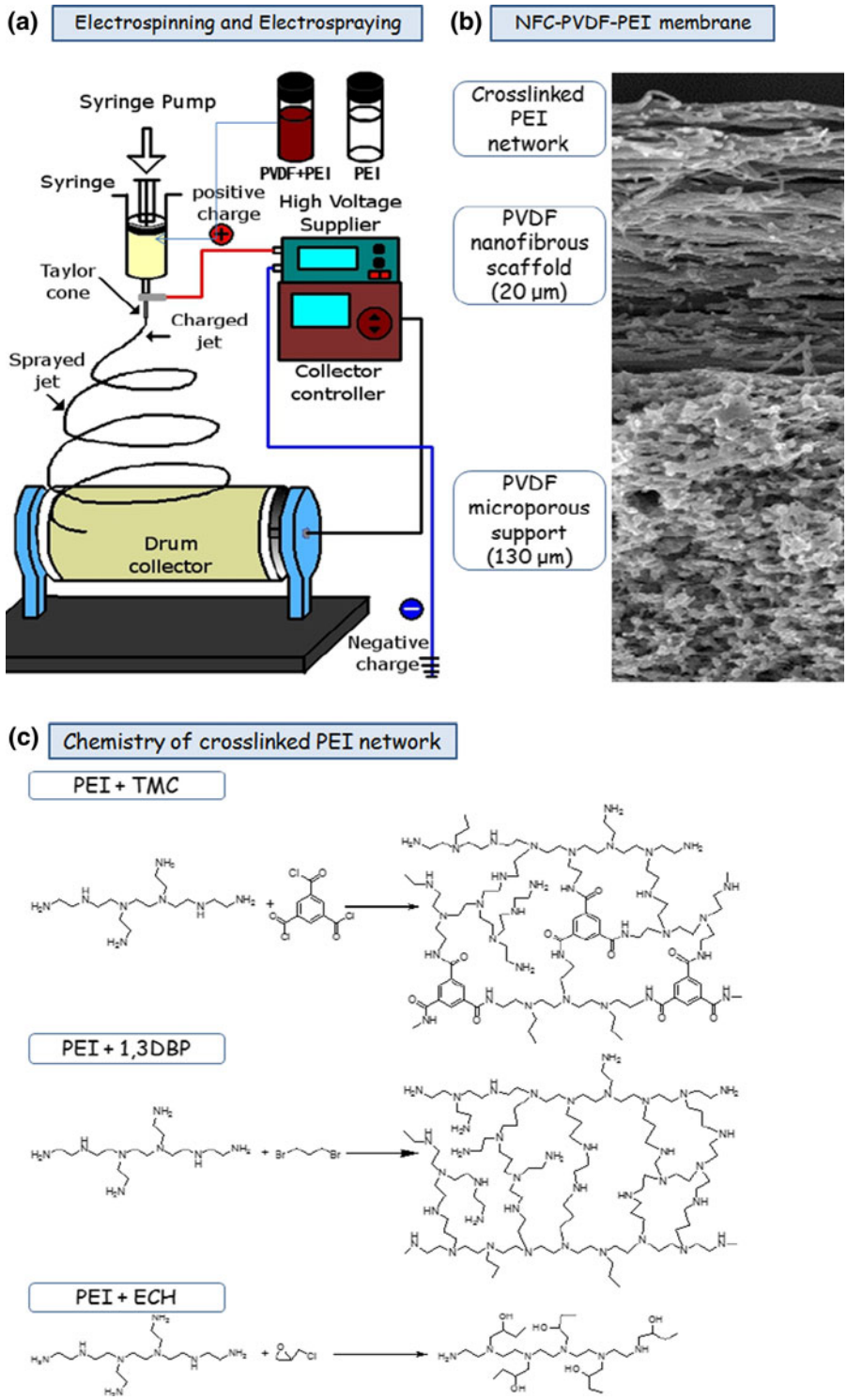

Fig. 1 Schematic diagram of the fabrication of nanofibrous composite (NFC–PVDF–PEI) membranes with PVDF microporous support, PVDF nanofibrous scaffolds, and crosslinked PEI networks

in toluene (1 % w/v) in a glass vessel at room temperature for 5 min (Fig. 1). Similarly, the NFC–PVDF–PEI-2 and NFC–PVDF–PEI-3 membranes were synthesized by reacting the PEI-coated PVDF nanofibrous scaffolds, respectively, with 20 wt% solutions of 1,3-DBP and ECH in toluene for 1 h at

Table 1 List of electrospinning and electrospraying process parameters

Process parameters	Electrospinning	Electrospraying
Concentration of polymer solution	18.5 % (w/w) PVDF and 2.5 % (w/w) PEI in a mixture (5:5 w/w) of DMF and NMP	Hyperbranched PEI (50 % w/w) in methanol
Amount of polymer solution (mL)	6	1
Solution flow rate (mL/h)	0.7	0.3
Applied voltage (kV)	29	29
Needle diameter (mm)	0.394	0.394
Needle collector distance (cm)	7.5	7.5
Drum collector speed (rpm)	500	2,500

45 °C. Following this, the membranes were rinsed three times with DI water and stored in DI water at room temperature.

Nanofiber and membrane characterization

The morphology, chemical composition, hydrophobicity, and zeta potential of the PVDF nanofibers and NFC–PVDF–PEI membranes were characterized using various analytical tools. The cross-sectional and surface morphologies of the nanofibers and membranes were imaged using a field emission scanning electron microscope (FESEM, FEI, SIRION-100, USA). Before imaging, all samples were coated with gold at 30 mA for 120 s to minimize the charging effect. To obtain the FESEM images, the membranes were frozen and fractured following immersion in liquid nitrogen. The SEM images were subsequently analyzed to estimate the thickness of the membrane surface layers using the ImageJ software (Abramoff et al. 2004). The compositions of the surface layers of the NFC–PVDF–PEI membranes were characterized by attenuated total reflectance-Fourier transform infrared spectroscopy (ATR-FTIR) using a JASCO 4100 FT-IR spectrometer (Japan). All samples were scanned from 500 to 4000 cm^{-1} with a scanning speed of 2 mm/s using a zinc selenide ATR crystal plate with an aperture angle of 45°. The hydrophobicity of each NFC–PVDF–PEI membrane was determined from contact angle measurements using a Phoenix 300 contact angle analyzer (SEO cooperation, Korea). A microsyringe was utilized to place a water droplet on the surface of each membrane. After 30 s, the image was captured and analyzed using the instrument's image processing software. Each reported contact angle is the average of 10 different measurements. The zeta potentials of the membranes were determined using the electrophoresis method (Shim et al. 2002). This involves measuring the electrophoretic mobility of monitoring particles inside an electrophoresis chamber consisting of a membrane and quartz cells (Shim et al. 2002). Due to the sorption and accumulation of ions at the surface of the membranes, an electro-osmotic flow occurs inside the electrophoresis chamber. This induced electro-osmotic flow causes the particles to undergo electrophoretic flow (Shim et al. 2002). An ELS-8000 electrophoretic light scattering spectrophotometer with a plate quartz cell (Otsuka Electronics, Japan) was employed to measure the electrophoretic mobility of the monitoring particles in 0.01 M KCl solutions as a function of pH. The monitoring particles consisted of PS latex particles (Otsuka Electronics, Japan) with a hydroxy propyl cellulose surface coating and diameter of 520 nm. The PS particles were dispersed in 0.01 N KCl solutions. The pH of the KCl solutions was adjusted with 0.1 N HCl or KOH as needed. The measured electrophoretic mobilities (U) [$cm^2/(V\ s)$] were employed to calculate the zeta potentials (ζ_{EP}) (mV) of the membranes using the Smoluchowski equation as given below (Shim et al. 2002):

$$\zeta_{EP} = 4\pi\eta U/\varepsilon_r\varepsilon_0 \quad (1)$$

where η is the liquid viscosity (0.89×10^{-3} Pa s), ε_r is the relative permittivity of liquid (78.38), and ε_0 is the vacuum permittivity (8.854×10^{-12} s m^{-1}).

Filtration experiments

A costume-built cross-flow filtration system with an effective membrane area of 24 cm^2 was employed to measure the salt rejection and permeate flux of each NFC–PVDF–PEI membrane. During each filtration

experiment, we used a feed solution of 10 L with a salt concentration of 2,000 mg/L. The pH of the feed solution was adjusted with a solution of 0.1 N HCl or 0.1 N NaOH as needed. All filtration experiments were carried out at room temperature and at a constant pressure of 7.0 bar. The salt rejection (R) of each membrane was assayed by electric conductivity measurements. R was expressed as:

$$R = \left(1 - C_p/C_f\right) \times 100 \quad (2)$$

where C_f and C_p are, respectively, the conductivity of the feed and permeate solutions. The permeate flux [J] (L m^{-2} h^{-1}) at time t through each membrane was expressed as:

$$J = V_p/(A \times \Delta t) \quad (3)$$

where V_p is the volume of permeate (L) collected during the sampling time Δt (h) and A is the effective membrane (m^2).

Results and discussion

Nanofiber synthesis and characterization

Hyperbranched PEI and PVDF were utilized, respectively, as building blocks for the ion-selective networks, nanofiborous scaffolds, and microporous supports of our new NFC membranes (Fig. 1). Due its high density of reactive amine groups and ready availability from commercial sources (Frechet et al. 2010; Diallo and Yu 2011), hyperbranched PEI is a versatile building block for preparing ion-selective thin films and networks. Recent studies have shown that hyperbranched PEI can be used to synthesize NF membranes with positively charged separation layers (Ba et al. 2009; Chiang et al. 2009; Sun et al. 2011). The selection of PVDF as base polymer to fabricate the nanofibrous scaffolds and microporous supports of the NFC membranes was motivated by two key considerations. First, PVDF is widely used as base polymer in the fabrication of commercial UF/MF membrane because of its high thermal/chemical resistance and tensile strength (Oh et al. 2009; Choi et al. 2011). Second, PVDF is soluble in a broad range of solvents including DMF, NMP, and dimethyl acetamide (DMAc) (Gopal et al. 2006; Choi et al. 2011). This provides many degrees of freedom for optimizing the properties of the microporous supports and nanofibrous scaffolds of our new NFC membranes (Fig. 1) by selecting the appropriate synthesis conditions. However, proteins and other hydrophobic macromolecular assemblies present in water/wastewater can easily foul PVDF membranes due to their hydrophobicity. Compared to membrane surface treatment methods such as chemical oxidation, plasma treatment and polymer grafting (Strathmann 2011), blending hydrophobic polymers such as PVDF with more hydrophilic polymers is versatile and easy to implement method for decreasing the hydrophobicity of polymeric membranes (Mansouri et al. 2010). Because hyperbranched PEI and PVDF are both soluble in DMF and NMP, we utilized blends of PVDF (18.5 wt%) and PEI (2.5 wt%) to synthesize the nanofibrous scaffolds of the NFC–PVDF–PEI membranes (Fig. 1). The blends were prepared by dissolving the required amounts of PVDF and PEI in mixtures of DMF and NMP (1:1 w/w). Consistent with literature data (Ramakrishina et al. 2005), we found that the average diameter (155.8 ± 44.4 nm) of PVDF nanofibers electrospun using mixtures DMF/NMP (1:1 w/w) was larger than that of the corresponding PVDF

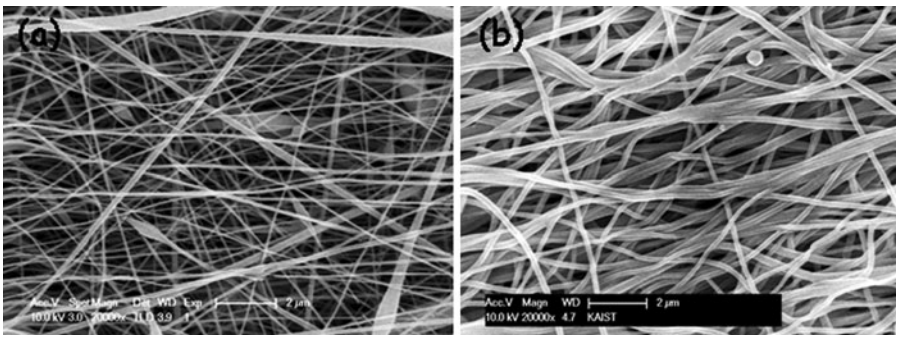

Fig. 2 Electrospun nanofiber from polymer solution dissolved in **a** DMF solvent and **b** NMP/DMF mixed solvent

nanofibers (81.4 ± 21.4 nm) that were prepared using pure DMF (Fig. 2).

The utilization of mixtures of as ES solvents provides several advantages (Ramakrishina et al. 2005; Yung et al. 2010). First, this can eliminate the formation of beaded nanofibers (Ramakrishina et al. 2005). Beads are defects that are formed during the ES of PNFs when low viscosity solvents are utilized to dissolve the base polymers (Ramakrishina et al. 2005). In NFC membranes, beaded nanofibers decrease the membrane porosity and interrupt the flow of water through the membrane nanofibrous scaffolds (Ramakrishina et al. 2005). Note that the viscosity of NMP (1.7 cps) is larger than that of DMF (0.9 cps). Consistent with the observations of Ramakrishina et al. (2005), we have found the use of pure DMF as spinning solvent resulted in the formation of beaded PVDF nanofibers (Fig. 2a). In contrast, no beaded nanofibers were observed when mixtures of DMF and NMP (1:1 w/w) were utilized as spinning solvents (Fig. 2b). Second, the use of mixtures as spinning solvents can also increase both the adhesion/tensile strength of PNFs as well as the strength of their adhesion to nonwoven microporous supports. Yung et al. (2010) have investigated the adhesion/tensile strength of PNFs and their delamination from nonwowen microporous polymeric supports. They reported that the adhesion between poly(ethersulfone) (PES) nanofibrous layers and a nonwoven poly(ethylene terephthalate) (PET) microporous support was stronger when the base PES polymer was dissolved in mixtures of DMF and NMP (6:4 w/w). We have also found that the use of mixtures of DMF and NMP increases the adhesion strength of PVDF nanofibers to PVDF microporous supports. Consistent with the observations of Yung et al. (2010), we have found the use of pure DMF as spinning solvent resulted in the formation of PVDF nanofibrous scaffolds that are easily peeled off by hand from the PVDF microporous supports. In contrast, none of the PVDF nanofibrous scaffolds could be peeled off by hand from their supports when the fibers were electrospun using mixtures of DMF and NMP (1:1 w/w).

Membrane synthesis and characterization

To fabricate our new ion-selective NFC membranes (Fig. 1), we first employed electrospraying to deposit films of hyperbranched PEI onto PVDF nanofibrous scaffolds that were electrospun onto commercial PVDF MF membrane supports using 1:1 w/w mixtures of DMF + NMP. Electrospraying has emerged as a versatile technique for depositing films onto a broad range of substrates including polymeric membranes (Jaworek and Sobczyk 2008). These films can be deposited from solutions or suspensions of microparticles/nanoparticles with controlled thickness ranging from 10 nm to 100 μm. Rosso et al. (2008) have successfully combined ES with electrospraying to fabricate novel catalytic membranes consisting of polysulfone nanofibrous scaffolds with embedded TiO_2 nanoparticles. Table 1 shows the process parameters used to spray the PVDF nanofibrous scaffolds with hyperbranched PEI. Based on SEM images (data not shown), we found that we can fully cover the surfaces of the PVDF nanofibrous scaffolds by spraying them with 1.0 mL of a 50 wt% solution of PEI in methanol. Following electrospraying, the PEI-laden nanofibrous PVDF were reacted, respectively, with TMC, 1,3-DBP, and ECH to produce NFC membranes with crosslinked PEI networks (Fig. 1) as described in the section "Experimental methods and procedures." Table 2 shows selected properties of the NFC–PVDF–PEI membranes that were measured in this study including contact angle, zeta potential, isoelectric point, and surface layer thickness. Figure 4 shows the FESEM images of the surface and cross-section morphology of the NFC–PVDF–PEI membranes. As shown in Fig. 4a and b, the surface of the NFC–PVDF–PEI-1 membrane (with TMC crosslinker) consists of a film of PVDF nanofibers with crosslinked PEI macromolecules. Due to its rough/wiggly surface morphology, it was difficult to measure the thickness of the surface layer of the NFC–PVDF–PEI-1 membrane with high precision. Using the ImageJ software (Abramoff et al. 2004), we estimate the thickness of the membrane surface layer is equal to 240 ± 100 nm (Table 2). This value is within the range of the observed thickness (150–2,000 nm) of the surface layers of conventional polymeric NF membranes (Baker 2004; Ji et al. 2011). Figure 3 shows that both the surface of the NFC–PVDF–PEI-2 membrane (with DBP crosslinker) and that of the NFC–PVDF–PEI-3 membrane (with ECH crosslinker) consist also of films of PVDF nanofibers with crosslinked PEI macromolecules. We estimate the thickness of the separation layers of the NFC–PEI-2 and NFC–PEI-3 membranes are, respectively, equal to 10 and 13 μm (Table 2). We

Table 2 Selected properties of the NFC–PVDF–PEI membranes synthesized in this study

Membrane	Surface layer	Contact angle[a]	Isoelectric point	Zeta potential (pH 6)	Surface layer thickness
NFC–PVDF–PEI-1	Crosslinked PEI/TMC	38.6 ± 1.4°	7.8	39.7 ± 3.7 mV	240 ± 100 nm
NFC–PVDF–PEI-2	Crosslinked PEI/DBP	54.9 ± 0.5°	6.4	9.0 ± 3.0 mV	10 μm
NFC–PVDF–PEI-3	Crosslinked PEI/ECH	50.2 ± 1.3°	5.7	−4.5 ± 0.9 mV	13 μm

[a] All the contact angles were measured in water. The contact angle of the PVDF MF membrane support is equal to 130.2 ± 0.9°

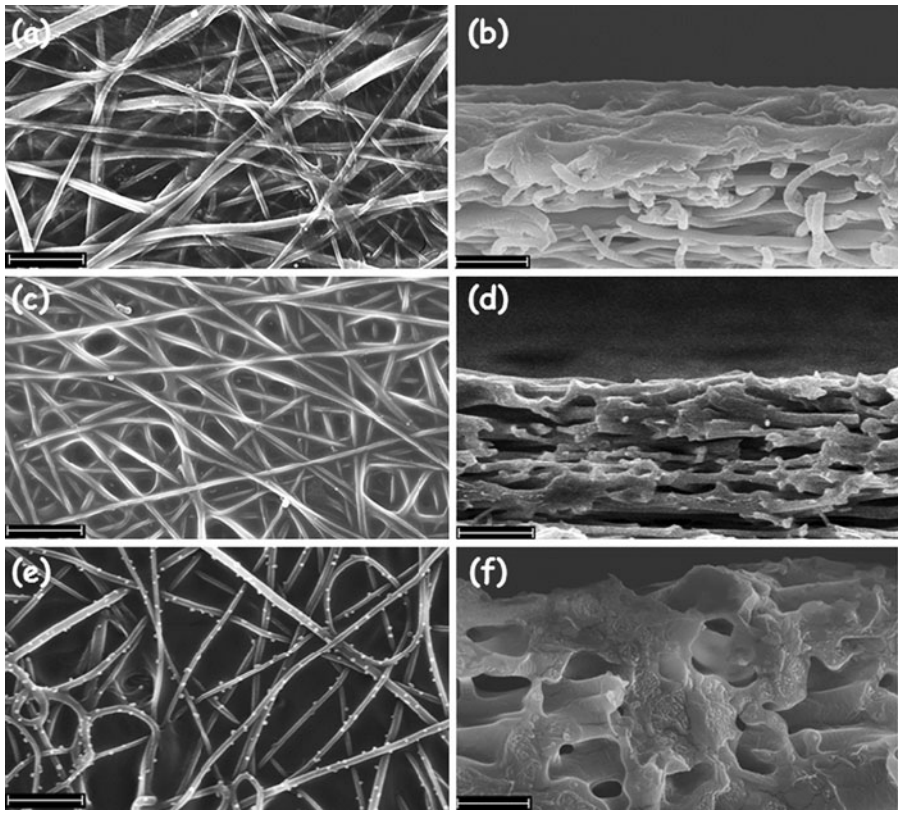

Fig. 3 FE-SEM images of the surfaces and cross-section morphologies of an NFC–PEI-1 membrane crosslinked with trimeosyl chloride (**a**, **b**), NFC–PEI-2 membrane crosslinked with 1,3-dibromopropane (**c**, **d**), and NFC–PEI-3 crosslinked with epichlrohydrin (**e**, **f**). The length of the scale bar in each panel is equal to 5 μm

attribute the large thickness of the surface of these membranes to longer crosslinking reaction times (1 h) at higher temperature (45 °C) in the presence of excess reagents (i.e., solutions of 20 wt% of DBP/ECH in toluene).

Figure 4 shows the ATR-FTIR spectra of a PDVF membrane support, a blended PVDF/PEI nanofibrous scaffold and those of the NFC–PVDF–PEI membranes. Figure 3a highlights several characteristic peaks of PVDF surfaces including CF_2 bending (615 and 766 cm^{-1}), CH_2 rocking (840 cm^{-1}), CH stretching (976 cm^{-1}), and CF stretching (1234 and 1279 cm^{-1}) (Bormashenko et al. 2004). Figure 3b shows that the blended PVDF/PEI nanofibrous scaffold exhibits two major peaks including (i) NH_2 bending (1655 cm^{-1}) from primary amines and (ii) NH stretching (3255 cm^{-1}) from primary/secondary amines. We assign these peaks to PEI macromolecules that are embedded inside PVDF nanofibrous scaffold (Fig. 1). As shown in Fig. 4c, the FT-IR spectrum of the NFC–PVDF–PEI-1 membrane exhibits some characteristic features of NF membranes with

amide groups including CN stretching (1641 cm^{-1}) and C=O stretching (1532 cm^{-1}) (Setiawan et al. 2011; Sun et al. 2011). These amide groups are generated when the PEI macromolecules that are embedded in the membrane PVDF nanofibrous scaffold react with TMC molecules (Fig. 1). Note that the FT-IR spectrum of the NFC–PVDF–PEI-2 membrane (Fig. 4d) shows no new characteristic peak. This observation is consistent with the fact that mostly secondary/tertiary amines are generated when the embedded PEI macromolecules of the membrane PVDF nanofibrous scaffold reacts with 1,3-DBP molecules (Fig. 1). In contrast, the FT-IR spectrum of the NFC–PVDF–PEI-3 membrane exhibits a new peak, i.e., OH stretching at 3257 cm^{-1} indicating that hydroxyl groups are produced when the PEI macromolecules that are embedded inside the membrane PVDF nanofibrous scaffold reacts with ECH molecules (Fig. 1). Table 2 shows significant differences between the hydrophilicity and zeta potential potentials of NFC–PVDF–PEI membranes. Note that the contact angle of the PVDF membrane support is equal to 130.2 ± 0.9° thereby indicating that the support is very hydrophobic. In contrast, the contact angles for the NFC–PVDF–PEI-1, NFC–PVDF–PEI-2, and NFC–PVDF–PEI-3 membranes are equal, respectively, to 38.6 ± 1.4°, 54.9 ± 0.5°, and 50.2 ± 1.3° thereby suggesting these membranes are hydrophilic and less susceptible to fouling via sorption of proteins and other hydrophobic macromolecular assemblies present in water/wastewater. It is worth mentioning that the contact angle of the NFC–PVDF–PEI-1 membrane (38.6 ± 1.4°) is smaller by ~10–20° than those of commercial TFC PA NF/RO membranes with crosslinked PA separation layers. These membranes have contact angles of 50–60° (Elimelech and Philipp 2011). Figure 5 shows the zeta potentials of the NFC–PVDF–PEI membranes measured at various pH. Table 2 shows their estimated isoelectric points and zeta potentials. The isoelectric points of the NFC–PVDF–PEI-1, NFC–PVDF–PEI-2, and NFC–PVDF–PEI-3 membranes are, respectively, equal to 7.8, 6.4, and 5.7. Their zeta potentials at pH 6 are equal to 39.7 3.7, 9.0 ± 3.0, and −4.5 ± 0.9 mV, respectively.

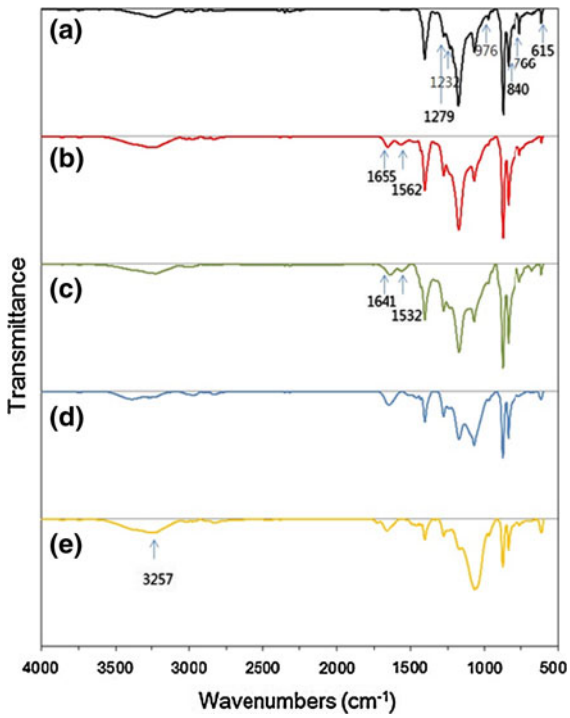

Fig. 4 FTIR-ATR spectra of a PVDF microporous support (**a**), a PVDF + PEI nanofibrous scaffold (**b**), NFC–PVDF–PEI-1 membrane crosslinked with trimeosyl chloride (**c**), NFC–PVDF–PEI-2 membrane crosslinked with 1-3 dibromopropane (**d**), and NFC–PVDF–PEI-3 membrane crosslinked with epichlorohydrin (**e**)

Evaluation of membrane performance

The overall results of the characterization experiments indicate that the NFC–PVDF–PEI-1 membrane (with TMC crosslinker) is more hydrophilic than commercial TFC-PA RO/NF membranes. The large and positive zeta potential of the NFC–PVDF–PEI-1 membrane at pH 6–7 (Fig. 5) suggests that it has good potential for high water flux and improved rejection for monovalent cations. To evaluate the performance of this new membrane, we carried out

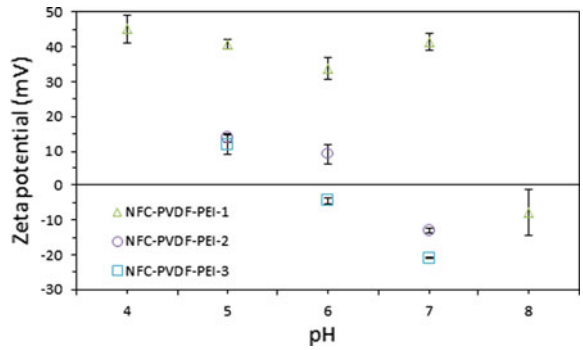

Fig. 5 Zeta potentials of NFC–PEI membranes at various pH values

cross-flow filtration experiments to measure its ion rejection and permeate flux in saline solutions as described in the section "Experimental methods and procedures." Aqueous solutions (2,000 mg/L) of four salts (NaCl, $MgCl_2$, Na_2SO_4, and $MgSO_4$) were evaluated. Figure 6 shows the salt rejection and permeate flux of the NFC–PVDF–PEI-1 membrane during the course of a typical 12 h filtration experiment. In all cases, we found that the membrane salt rejection and permeate flux reached constant values after 2 h of filtration. Figure 7 shows that the NFC–PVDF–PEI-1 membrane exhibits higher rejections for the 2-1 salt ($MgCl_2$) and 2-2 salt ($MgSO_4$) than for the 1-1 salt (NaCl) and 1-2 salt (Na_2SO_4) at pH 4 and 6. This rejection profile is consistent with that of a Donnan exclusion membrane with a positive surface charge (Schäefer et al. 2005). As indicated in Table 1, the NFC–PVDF–PEI-1 membrane has an isoelectric point of 7.8. The isoelectric point of a membrane is the pH at which it has no net charge in solution. Thus, the

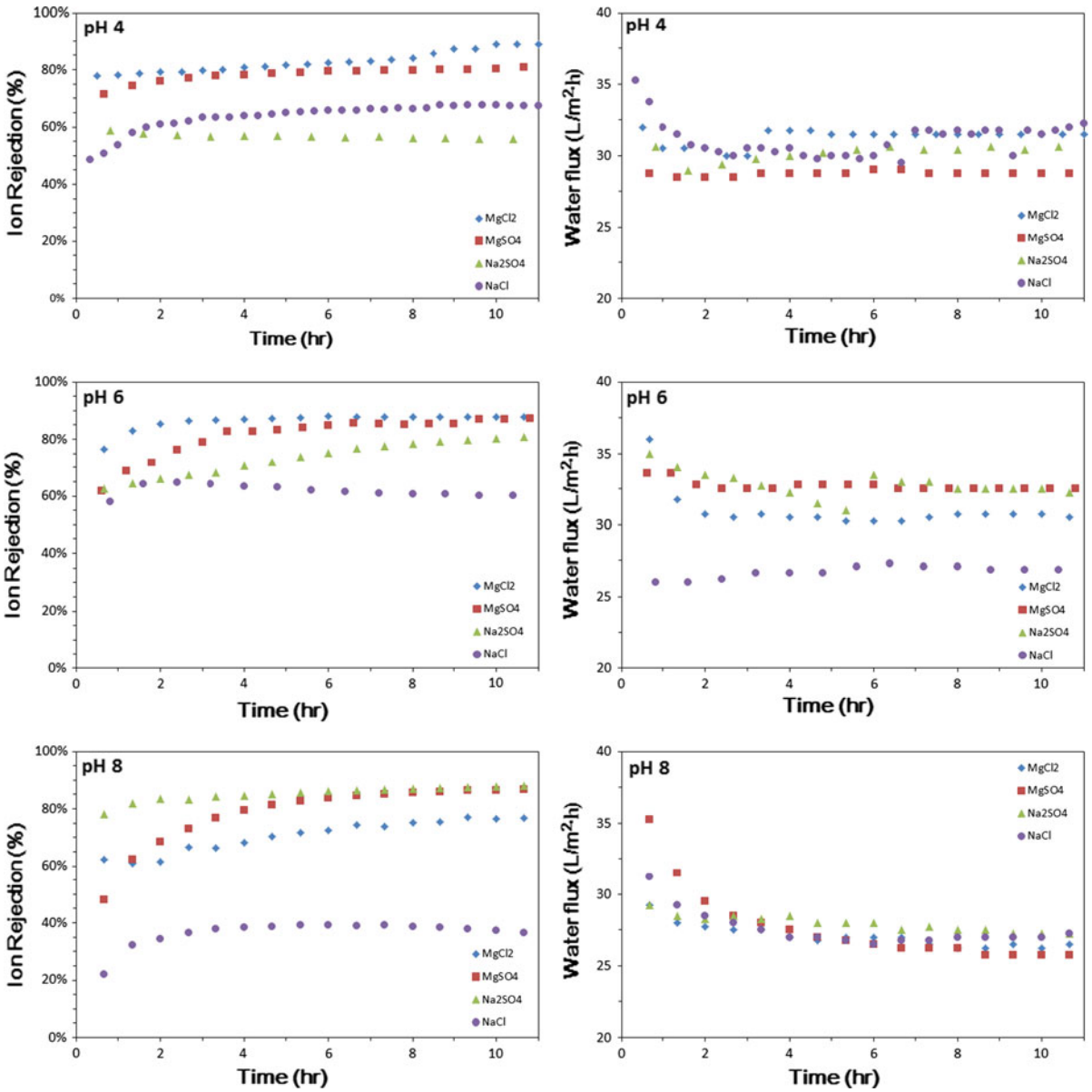

Fig. 6 Ion rejection and water flux of NFC–PEI-1 at pH 4, 6, and 8 as a function of time at room temperature. A cross-flow filtration system was utilized to measure the ion rejection and permeate flux of the membrane

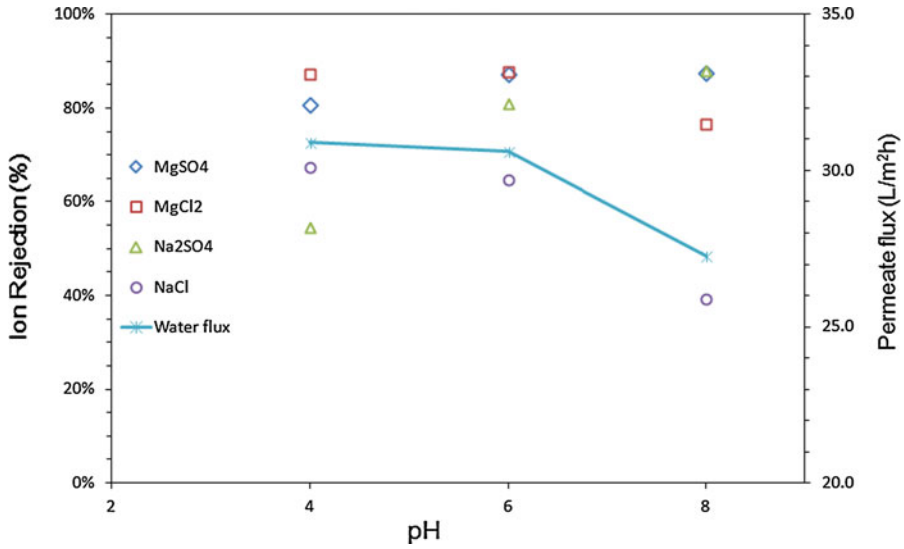

Fig. 7 Salt rejection and water flux for NFC–PEI-1 membrane as a function of pH at room temperature

NFC–PVDF–PEI-1 membrane is (i) positively charged at pH 4 and 6 and (ii) negatively charged at pH 8 (Fig. 6). Consistent with the Donnan effect, the NFC–PVDF–PEI-1 membrane will have a higher rejection for divalent cations (e.g., Mg^{2+}) over monovalent cations (e.g., Na^{+}) at pH 4 and 6 (Schäefer et al. 2005; Escoda et al. 2010; Déon et al. 2011). Note that a positively charged membrane will also reject an equivalent amount of anions to maintain overall solution electroneutrality. Because of this, we expect the rejection of a magnesium salt (e.g., $MgCl_2$ and $MgSO_4$) by a NFC–PVDF–PEI-1 membrane will be larger than that of a sodium salt (e.g., Na_2SO_4) in aqueous solutions at pH 4 and 6. At pH 8, however, Fig. 7 shows that the salt rejection order of the NFC–PVDF–PEI-1 membrane is $Na_2SO_4 > MgCl_2 >$ NaCl. We found that the $MgCl_2$ rejection of the NFC–PVDF–PEI-1 membrane decreased from 87.2 to 76.7 % as solution pH water increased from 4 to 8. In contrast, its Na_2SO_4 rejection increased significantly from 54.5 to 88.0 % with increasing pH from 4 to 8. At pH 8, the rejection of $MgSO_4$ (87.4 %) is comparable to that of Na_2SO_4 (88.0 %). However, it is significantly larger than that (76.7 %) of $MgCl_2$ at pH 8. The observed higher rejections of Na_2SO_4 and $MgSO_4$ by the NFC–PVDF–PEI-1 membrane are also consistent with those of Donnan exclusion membranes with negative surface charges including TFC PA NF membranes (Schäefer et al. 2005; Verissimo et al. 2005; Pontié et al. 2008) and sulfonated polyethersulfone asymmetric NF membranes (Tsuru et al. 1991; Schaep et al. 1998).

We also measured the salt rejections and permeate fluxes of the NFC–PVDF–PEI-2 and NFC–PVDF–PEI-3 membranes (Table 3). Table 3 shows the $MgCl_2$/NaCl rejections and permeate fluxes of the NFC–PVDF–PEI membranes at pH 6. The $MgCl_2$/NaCl rejections and permeate fluxes of selected NF membranes with positively charged surface layers are also listed in Table 3 (Ji et al. 2011). As shown in Table 3, the $MgCl_2$ rejection of the NFC–PVDF–PEI-1 membrane (87.8 %) is higher than those of the NFC–PVDF–PEI-2 membrane (75.5 %) and NFC–PVDF–PEI-3 membrane (76.4 %). Note that NaCl rejection of the NFC–PVDF–PEI-1 and NFC–PVDF–PEI-3 membranes are comparable. They are equal to 64.8 and 62.6 %, respectively. However, the NaCl rejection of the NFC–PVDF–PEI-2 is lower and equal to 22.9 %. Table 3 indicates that the permeate flux of the NFC–PVDF–PEI-3 membrane is relatively low (8–9.0 L m^{-2} h^{-1}). In contrast, the permeate flux of the NFC–PVDF–PEI-1 membrane is relatively high (27–30 L m^{-2} h^{-1}). As shown in Table 3, the permeate flux of the NFC–PVDF–PEI-2 membrane (25–30 L m^{-2} h^{-1}) is comparable to that of the NFC–PVDF–PEI-2 membrane. This result is surprising as the NFC–PVDF–PEI-1 membrane has a higher surface charge at pH 6 (39.7 mV versus 9.0 mV) with a lower contact angle (38.6° versus 54.9°) and a thinner surface layer (200 nm versus 10 μm). At the

Table 3 Comparative test results of ion rejection and water flux for positively charged nanofiltration membranes (modified from Ji et al. 2011)

Membrane	R_{MgCl_2} (%)	J_{MgCl_2} (L m^{-2} h^{-1})	R_{NaCl} (%)	J_{NaCl} (L m^{-2} h^{-1})	Separation layer	Experimental conditions	Reference
NFC–PVDF–PEI-1	87.8	30.5	64.8	27.1	Crosslinked PEI/TMC	2,000 ppm $MgCl_2$; 2,000 ppm NaCl; 7.0 bar	This study
NFC–PVDF–PEI-2	75.5	29.8	22.9	24.8	Crosslinked PEI/1,3-DBP	2,000 ppm $MgCl_2$; 2,000 ppm NaCl; 7.0 bar	This study
NFC–PVDF–PEI-3	76.4	9.3	62.6	8.0	Crosslinked PEI/ECH	2,000 ppm $MgCl_2$; 2,000 ppm NaCl; 7.0 bar	This study
PPO	73.0	63.0	36.0	63.0	Poly(2,6-dimethyl-1,4-phenylene oxide)	1,000 ppm $MgCl_2$; 1,000 ppm NaCl; 3.5 bar	Tongwen and Weihua (2003)
PDMAEMA/PSF	98.0	8.3	77.8	7.6	Poly(*N*,*N*-dimethylaminoethyl methacrylate)	1,000 ppm $MgCl_2$; 1,000 ppm NaCl; 8.0 bar	Du and Zhao (2004)
HACC/PAN NF-1	94.1	6.9	47.3	12.9	2-hydroxypropyltrimethyl ammonium chloride chitosan/hexane diacid/acetic anhydride	2,000 ppm $MgCl_2$; 2,000 ppm NaCl; 5.0 bar	Huang et al. (2008)
QAPPESK	84.0	49.0	31.0	54.0	Quaternized poly(phthalazinone ether sulfone ketone)	1,000 ppm $MgCl_2$; 1,000 ppm NaCl; 4.0 bar	Yan et al. (2008)
GCTACC/PAN	91.7	8.5	57.0	8.6	A graft copolymer of trimethylallyl ammonium chloride onto chitosan	2,000 ppm $MgCl_2$; 2,000 ppm NaCl; 12.0 bar	Huang et al. (2009)
PEI modified membrane	91.2	15.0	82.2	15.0	PEI coating on polyamide thin film composite membrane	75 ppm $MgCl_2$; 90 ppm NaCl; 8.0 bar	Zhou et al. (2009)
PCNFM3	94.3	19.1	60.7	20.6	Poly(2-methacryloyloxy ethyl trimethylammonium chloride-co-2-hydroxyethyl acrylate)	1,000 ppm $MgCl_2$; 1,000 ppm NaCl; 6 bar	Ji et al. (2011)
M-40	63.3	30.2	36.6	30.2	Poly(arylene ether sulfone) with pendant tertiary amine group	1,000 ppm $MgCl_2$; 1,000 ppm NaCl; 5 bar	Zhang et al. (2011)

present time, we have no definite explanation for this observation. The overall results of our study suggest that NFC membranes with PVDF nanofibrous scaffolds and crosslinked PEI networks are promising building blocks for the fabrication of high performance NF membranes for water purification. Without optimization, our new NFC–PVDF–PEI-1 membrane (Fig. 1) already exhibit a high water flux ($\sim$30 L m^{-2} h^{-1}) and good rejections for $MgCl_2$ ($\sim$88 %) and NaCl ($\sim$65 %) rejection in salt solutions (2,000 mg/L) at pH 6 using a pressure of 7 bar (Table 3). It is worth mentioning that the all the nanofiltration membranes listed in Table 3 that have higher $MgCl_2$/NaCl rejections than those of NFC–PVDF–PEI-1 membrane have also lower permeate fluxes ($\sim$15.0–19.0 L m^{-2} h^{-1}). Additional experiments are being carried out to improve the performance of the NFC–PVDF–PEI membranes (Fig. 1).

Summary and conclusions

In this study, we described the synthesis of a new generation of NFC membranes for water purification. These new NFC membranes consisted of crosslinked hyperbranched PEI networks supported by PVDF

nanofibrous scaffolds that were deposited onto commercial PVDF MF membrane supports. To fabricate these new NFC membranes, we first utilized ES to deposit blends of PVDF/PEI nanofibers onto commercial PVDF MF membranes. Following completion of the ES process, we deposited films of hyperbranched PEI onto PVDF nanofibrous scaffolds using electrospraying. The PEI-laden nanofibrous PVDF scaffolds were then reacted with TMC, 1,3-DBP, and ECH, respectively, to produce NFC membranes with crosslinked PEI separation layers. The morphology, composition, hydrophobicity, and surface charge of the new NFC–PVDF–PEI membranes were subsequently characterized using FESEM, ATR-FTIR, contact angle, and zeta potential measurements. The salt rejection and permeate flux of the new membranes were evaluated using a costume-built filtration system with an effective membrane area of 24 cm^2. During each filtration experiment, we used a feed solution of 10 L with a salt concentration of 2,000 mg/L. The pH of the feed solution was adjusted with a solution of 0.1 N HCl or 0.1 N NaOH as needed. All filtration experiments were carried out at room temperature and at a constant pressure of 7.0 bar. Aqueous solutions (2,000 mg/L) of four salts (NaCl, $MgCl_2$, Na_2SO_4, and $MgSO_4$) were evaluated. We found that our NFC–PVDF membrane with crosslinked PEI/TMC networks has a high water flux ($\sim$30 L m^{-2} h^{-1}) and high rejections for $MgCl_2$ ($\sim$88 %) and NaCl ($\sim$65 %) at pH 6 using a pressure of 7 bar. The overall results of our study suggest that PVDF nanofibers and hyperbranched PEI are promising building blocks for the fabrication of high performance NF membranes for water purification.

Acknowledgments This study was carried out at Korea Advanced Institute of Science and Technology (KAIST) and at the California Institute of Technology (Caltech). Selected materials characterization studies (zeta potential measurements) were carried out at the Gwangju Institute of Science and Technology (GIST). Funding for KAIST was provided by the EEWS Initiative (NT080607C0209721). Funding for Caltech was provided by the U.S National Science Foundation (NSF) [CBET EAGER Award 0948485]. W. A. Goddard III was supported partially by the KAIST World Class University (WCU) program (NRF-31-2008-000-10055).

References

Abramoff MD, Magalhaes PJ, Ram SJ (2004) Image processing with ImageJ. Biophotonics Int 11:36–42

Ba C, Langer J, Economy J (2009) Chemical modification of P84 copolyimide membranes by polyethylenimine for nanofiltration. J Membr Sci 327:49–58

Baker RW (2004) Membrane technology and applications, 2nd edn. Wiley, Chichester

Bormashenko Y, Pogreb R, Stanevsky O, Bormashenko E (2004) Vibrational spectrum of PVDF and its interpretation. Polym Test 23:791–796

Cheng S, Oatley DL, Williams PM, Wright CJ (2011) Positively charged nanofiltration membranes: review of current fabrication methods and introduction of a novel approach. Adv Colloid Interface Sci 164:12–20

Chiang Y-C, Hsub Y-Z, Ruaan R-C, Chuang C-J, Tung K-L (2009) Nanofiltration membranes synthesized from hyperbranched polyethyleneimine. J Membr Sci 326:19–26

Choi H, Kwon Y, Jung Y, Hong S, Tak T (2011) Preparation and characterization of antifouling poly(vinylidene fluoride) blended membranes. J Appl Polym Sci 123:286–291

Déon S, Escoda A, Fievet P (2011) A transport model considering charge adsorption inside pores to describe salts rejection by nanofiltration membranes. Chem Eng Sci 66:2823–2832

Diallo MS, Brinker JC (2011) Nanotechnology for sustainability: environment, water, food, minerals and climate. In: Roco MC, Mirkin C, Hersham M (eds) Nanotechnology research directions for societal needs in 2020: retrospective and outlook. Science Policy Reports, Springer, pp 221–259

Diallo MS, Yu C (2011) Soluble anion exchangers from hyperbrannched macromolecules. US Patent Application Pub. No: 2011/0315636 A1

Du R, Zhao J (2004) Properties of poly (N,N-dimethylaminoethyl methacrylate)/polysulfone positively charged composite nanofiltration membrane. J Membr Sci 239:183–188

Elimelech M, Philipp WA (2011) The future of seawater desalination: energy, technology and the environment. Science 333:712–717

Escoda A, Lanteri Y, Fievet P, Déon S, Szymczyk A (2010) Determining the dielectric constant inside pores on nanofiltration membranes from membrane potential measurements. Langmuir 26:14628–14635

Frechet JMJ, Boz E, Diallo MS, Chi Y (2010) Extraction of anions from solutions and mixtures using hyperbranched macromolecules. US Patent Application No.: 20100181257

Gopal R, Kaur S, Ma ZW, Chan C, Ramakrishna S, Matsuura T (2006) Electrospun nanofibrous filtration membrane. J Membr Sci 281:581–586

Huang R, Chen G, Sun M, Gao C (2008) Preparation and characterization of quaterinized chitosan/poly(acrylonitrile) composite nanofiltration membrane from anhydride mixture cross-linking. J Membr Sci 58:393–399

Huang R, Chen G, Sun M, Gao C (2009) Preparation and characterization of composite NF membrane from a graft copolymer of trimethylallyl ammonium chloride onto chitosan by toluene diisocyanate cross-linking. Desalination 239:38–45

Jaworek A, Sobczyk AT (2008) Electrospraying route to nanotechnology: an overview. J Electrostat 66:197–219

Ji Y, An Q, Zhao Q, Chen H, Gao C (2011) Preparation of novel positively charged copolymer membranes for nanofiltration. J Membr Sci 376:254–265

Mansouri J, Harrisson S, Chen V (2010) Strategies for controlling biofouling in membranefiltration systems: challenges and opportunities. J Mater Chem 20:4567–4586

Oh SJ, Kim N, Lee YT (2009) Preparation and characterization of PVDF/TiO_2 organic–inorganic composite membranes for fouling resistance improvement. J Membr Sci 345: 13–20

Pontié M, Dach H, Leparc J, Hafsi M, Lhassani A (2008) Novel approach combining physico-chemical characterizations and mass transfer modelling of nanofiltration and low pressure reverse osmosis membranes for brackish water desalination intensification. J Membr Sci 221:174–191

Ramakrishina S, Fujihara K, Teo W-E, Lim T-C, Ma Z (2005) An introduction to electrospinning and nanofibers. World Scientific Publishing Co., Singapore

Rosso M, Sundarrajan S, Pliszka D, Ramakrishina S, Modesti M (2008) Multifunctional membranes based on spinning technologies: the synergy of nanofibers and nanoparticles. Nanotechonology 19:285707 (6 pp)

Schäefer A, Fane AG, Waite TD (2005) Nanofiltration: principles and applications. Elsevier, New York

Schaep J, Bruggen BVD, Vandecasteele C, Wilms D (1998) Influence of ion size and charge in nanofiltration. Sep Purif Technol 14:155–162

Service RF (2006) Desalination freshens up. Science 313:1088–1090

Setiawan L, Wang R, Li K, Fane AG (2011) Fabrication of novel poly(amide-imide) forward osmosis hollow fiber membranes with a positively charged nanofiltration-like selective layer. J Membr Sci 369:196–205

Shannon MA, Bohn PW, Elimelech M, Georgiadis J, Marinas BJ, Mayes A (2008) Science and technology for water purification in the coming decades. Nature 54:301–310

Shim Y, Lee HJ, Lee SY, Moon SH, Cho J (2002) Effects of natural organic matter and ionic species on membrane surface charge. Environ Sci Technol 36:3864–3871

Strathmann H (2011) Introduction to membrane science and technology. Wiley-VCH Verlag & Co, Weinheim

Sun SP, Hatton AT, Chung TS (2011) Hyperbranched polyethyleneimine induced cross-linking of polyamide-imide nanofiltration hollow fiber membranes for effective removal of ciprofloxacin. Environ Sci Technol 45: 4003–4009

Tongwen X, Weihua Y (2003) A novel positively charged composite membranes for nanofiltration prepared from poly(2,6-dimethyl-1,4-phenylene oxide) by in situ amines crosslinking. J Membr Sci 215:25–32

Tsuru T, Urairi M, Nakao S, Kimura S (1991) Negative rejection of anions in the loose reverse osmosis separation of mono- and divalent ion mixture. Desalination 81:219–227

UNEP (2006) Challenges to international waters—regional assessments in a global perspective. United Nations Environment Programme, Nairobi

Verissimo S, Peinemann KV, Bordado J (2005) New composite hollow fiber membrane for nanofiltration. Desalination 184:1–11

Vezzani D, Bandini S (2002) Donnan equilibrium and dielectric exclusion for characterization of nanofiltration membranes. Desalination 149:477–483

Wang X, Chen X, Yoon K, Fang D, Hsiao BS, Chu B (2005) High flux filtration medium based on nanofibrous substrate with hydrophilic nanocomposite coating. Environ Sci Technol 39:7684–7691

Yan C, Zhang S, Yang D, Jian X (2008) Preparation and characterization of chloromethylated/quaternized poly(phthalazinone ether sulfone ketone) for positively charged nanofiltration membranes. J Appl Polym Sci 107:1809–1816

Yoon K, Hsiao BS, Chu B (2008) Functional nanofibers for environmental applications. J Mater Chem 18:5326–5334

Yoon K, Hsiao BS, Chu B (2009) High flux ultrafiltration nanofibrous membranes based on polyacrylonitrile electrospun scaffolds and crosslinked polyvinyl alcohol coating. J Membr Sci 338:145–152

Yung L, Ma H, Wang X, Yoon K, Wang R, Hsiao BS, Chu B (2010) Fabrication of thin-film nanofibrous composite membranes by interfacial polymerization using ionic liquids as additives. J Membr Sci 365:52–58

Zhang Q, Wang H, Zhang S, Dai L (2011) Positively charged nanofiltration membrane based on cardo poly(arylene ether sulfone) with pendant tertiary amine groups. J Membr Sci 375:191–197

Zhou Y, Yu S, Gao C, Feng X (2009) Surface modification of thin film composite polyamide membranes by electrostatic self-deposition of polycations for improved fouling resistance. Sep Sci Technol 66:287–294